CONTROL OF EDGE PLATE STRAY GRAIN OF SINGLE-CRYSTAL TURBINE BLADE BY USING PROCESS BAR METHOD

Fei Qiu, Kun Bu, and Guoliang Tian
School of Mechanical Engineering, Northwestern Polytechnical University, Xi'an, Shaanxi, China

Bujingda Zheng
Department of Mechanical Engineering, The University of Melbourne, Parkville, VIC, Australia

https://doi.org/10.1007/s40962-019-00338-9

Abstract

Single-crystal (SX) turbine blade is the key component for aero-engines. However, the quality of the SX turbine blade is limited by the stray grain defects. When the structure and material are determined, in order to eliminate this defect, the process bar method is used to control the formation of stray grain. However, the structure of process bar is not researched. Generally, the process bar is designed by experience. In this paper, the simulation method is used to design the process bar structure. In order to describe the stray grain features, the critical stray grain cooling rate is put forward to predict the stray grain defect. With the help of the CAE analysis, the process bar dimension and position are determined by this method for a sample turbine blade. The result shows the process bar could modify the shape of the solidification interface and control the stray grain defect. Meanwhile, it also could control the dimension of the platform. And then, the effectiveness of this process bar design method is confirmed in the sample turbine blade experiment. The experiment result illustrated that the stray grain was eliminated.

Keywords: *single-crystal turbine blade, stray grain, process bar, investment casting, DD6 superalloy*

Introduction

Single-crystal (SX) turbine blade is the key component in aero-engines, and the integrity of the turbine blade's microstructure has an important influence on its mechanical properties. With the rapid development of high-efficiency turbine engines, the turbine blade have to withstand the higher operating temperature and harsher environments, putting forward the high demands on the performance of the turbine blade materials.[1] Due to the excellent mechanical behavior at high temperature, the SX superalloy blades are widely used in advanced aircraft engines and gas turbines. However, some types of crystal defects, such as freckles, stray grains, recrystallized grains and low-angle boundaries, can seriously affect the quality of SX turbine blade. According to the statistics result from the manufacturer, a significant number of the SX turbine blades were rejected due to stray grain defect.[2] Due to the increased demands for quality SX turbine blades, the method to eliminate the stray grain needs to be examined.

Current research shows that the mechanism of stray grain formation is based on dendritic arm melting or heterogeneous nucleation.[3] For dendritic arm melting, the main point is that the arm melting is formed at the beginning of the solidification process, and the solute enrichment or flow in the mushy zone would further lead to the breakage and shedding of the primary or higher dendrite arms. These breakages and shedding of the primary or higher dendrite arms are inconsistent with the original dendritic orientations.[4] However, the heterogeneous nucleation at the corner area of the platform may be cooled before that at the center of the test specimen. Due to the high cooling rate, the heterogeneous nucleation would start at the edge of the corner platform. At this state, the formation of the stray grain is not caused by the melting of the dendrite arms, but the heterogeneous nucleation, and the central area of the test specimen would then transform into the result of stray grain growth, initiating from the corners of the section platform.[5,6]

In the present research, Liu et al. presented a method to determine parameters for grain microstructure prediction, and it could be useful for predicting the stray grain defects.[7] Dein Ma[8,9] found that the stray grain can be controlled by adjusting the cooling rate. In the experiment, the graphite blocks were added to the edge platform area and the stray grain was eliminated. However, this method is difficult to apply in the industry. Szeliga[10] researched the effect of radiation baffle on mush zone, and the baffle significantly influences the predicted temperature distribution in the casting. It means this method could be used to adjust the gradient of mush zone, and it could be used to control the stray grain. However, this method is difficult to apply in the industry too. In addition, Xiaoli Zhang[11] showed that the refractory elements will increase the stray grain tendency. But this research cannot prove the stray grain is contributed by the Re-element. On the other hand, Yang Xiaoli et al.[12] used the CAFD method to research the effect of process parameters, and he proved that the stray grain area was increased with the rise of the withdrawal rates. Meyer[13] and Bussac[14] studied the stray grain formed mechanism and showed the thermal gradient and the withdrawal rate are the controlling parameters during a Bridgman furnace test. Their research showed that the way of controlling the stray grain should be focused on the nucleation undercooling. In addition, the grain continuators method is used to eliminate stray grain in Meyer's research. But the details of the grain continuators adding method are not introduced in his research. Meanwhile, Meng[3] researched the effect of platform dimension on the formation of stray grains, and his research shows the occurrence of stray grain increases with the rise of platform dimension.

According to literature review, present research for the control of stray grain concentrate more on the adjustment of the process parameters and elements of alloy. However, when the material of the turbine blade was determined, the only way to eliminate the stray grain is the process method, optimizing the process parameters or redesigning the structure of test specimen. In this research, the geometry of the test specimen was revised by adding a process bar, which is called, namely the process bar method. What is more, the process bar method is similar to the grain continuators method. Though the process method has been widely used in turbine blades, the process bar design method has not been researched. In this paper, the process bar structure is designed. Meanwhile, the simulation method is introduced to inform the process bar design. With the help of simulation method, the modified process bar was added to a turbine blade. Then, the experiment method was used to evaluate the simulation results.

Mechanism of Stray Grain Formation

The measurement of Critical Cooling Rate

As casting in the drawing process, the liquid isotherm near the side is higher than that in the middle of the channel.[15,16] This shape of liquid isotherm will induce stray grain when it is up to the cross-sectional area. And the mechanism of stray grain formation is shown in Figure 1. When the liquid interface comes to the side of the plate, the solidification begins as shown in Figure 1a. But the supercooling degree cannot satisfy the nucleation needs at this time. Generally, the critical nucleation supercooling degree (ΔT) is between liquid isotherm and solid isotherm. In order to describe the stray grain formation mechanism, supposing the distance between original dendrite and plate is H, the growing rate of the original dendrite is approximately equal to withdrawn rate (V), the length of the plate is L, and the growing rate of the dendrite which forms in the plate is V_2. When the side of the plate is up to the critical nucleation supercooling degree, the stray grain will form as shown in Figure 1b.

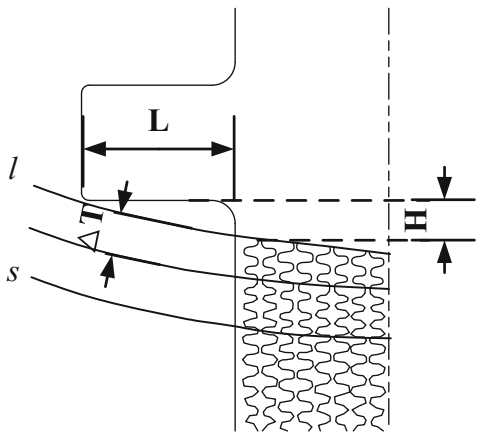

(a) undercooling at the corner of platform

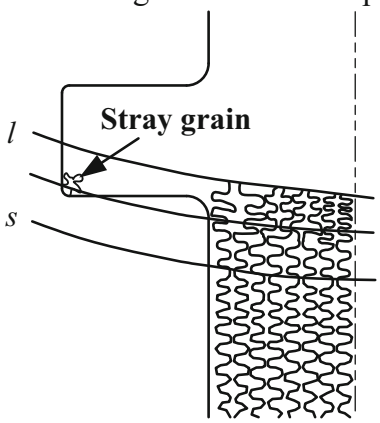

(b) nucleus formation of stray grain

Figure 1. Schematics of the formation of stray grain during directional solidification.

Thus, in order to predict the stray grain, the critical cooling rate (c) is measured. Suppose that the time when the platform corner reaches ΔT is t, the $t = \Delta T/c$. And the $c = G \cdot V$. The time when the original dendrite reaches the platform is $t_1 = H/V$. And if there is no stray grain formation, the original dendrite needs to fill up the whole platform. The time when the dendrite grows to the L is $t_2 = \int_0^L \frac{L}{V_2(\triangle T_i)} \mathrm{d}s$.[4] Thus, on the one hand, if the $t > t_1 + t_2$, there is no stray grain formation. On the other side, if the $t < t_1 + t_2$, the stray grain must exist. According to this principle, the stray grain prediction model can be expressed in Eqn. (1):

$$c_{sc} = \triangle T \Big/ \left(\frac{H}{V} + \int_0^L \frac{L}{V_2(\triangle T_i)} \mathrm{d}s \right) > c \qquad \text{Eqn. 1}$$

According to the above analysis, the C could be used to predict the stray grain formation. In this paper, in order to define the critical cooling rate, a statistical table is created from actual test results. As given in Table 1, when the V is out of 2.5 mm/min, stray grain easily forms at the turbine blade. Hence, when the V = 2.5 mm/min, the max cooling rate of the platform could be defined as the critical cooling rate. In order to determine the critical cooling rate, four thermo-couples were set at the corner of the platform. The temperature–time curve is recorded. And the critical cooling rate is the slope of the temperature–time curve at the solid temperature. The slope value is taken as absolute value. The maximum of the absolute slope value is determined as the critical cooling rate. The critical cooling rate was determined by actual experiments and defined as C_{sc} = 0.74029 °C/s.

Table 1. Statistics of Stray Grain Defects at Different V

V (mm/min)	Statistics of stray grain defects
2	NO
2.5	NO
3	Stray grain appear near the furnace wall
3.5	Stray grain appear near the furnace wall and the back of the turbine blade is forming stray grain
4	Stray grain appear near the furnace wall, the back of the turbine blade is forming stray grain and the body of the turbine blade appeared stray grain
5	The stray grain defects are obviously at the platform

Mechanism of Stray Grain Formation by Process Bar Method

According to the analysis of stray grain formation mechanism at the corner of platform, the principle of eliminating stray grain is changing the solidification interface. The most efficient method is modifying the elements of the superalloy or optimizing the cast structure. However, this is not the only way to adjust the solidification interface. The process method is also useful such as the adding graphite blocks method which had been proved by Ma.[6] Though the process bar method was already used in the investment casting, there is no research on the process bar adding principle.

With the help of the process bar, the cooling rate of the connecting area is reduced, which is due to the process bar that introduced a thermal node, and the heat loss rate is then reduced. Thus, the shape of nucleation isotherm is changed, and the stray grain can hardly form. The mechanism of stray grain formation by process bar method is shown in Figure 2. When the corner of the platform reaches the nucleation temperature the second dendrite arm

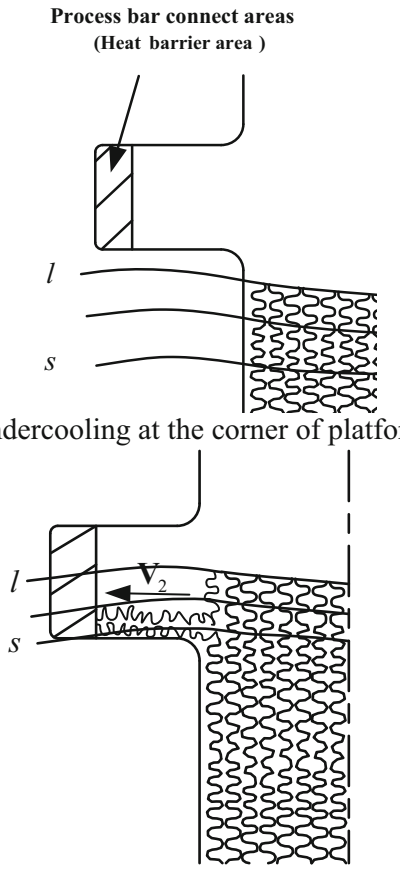

(a) undercooling at the corner of platform

(b) nucleus formation at the corner of platform

Figure 2. The mechanism of process bar.

is already growing to the corner, the new nucleation is limited, thus the platform grain is same as the body of the turbine blade.

Methodology

The Simulation Boundary Conditions

In order to obtain the precise thermal field, heat exchange coefficient between the shell mold and test specimen needs to be considered, as it is important for simulating directional investment casting. The results of casting–chill plate interface heat transfer coefficient are presented in Figure 3, which were acquired by measuring the temperature of the turbine blade during the investment casting.[17] The casting process was simulated by ProCAST under the ideal heat transfer assumption, procedures of which include temperature/time boundary conditions and properties of temperature-dependent materials. These parameters need to be assigned after being calculated. For the simulation, DD6 (Table 2) superalloy was selected. The shell mold and ceramic core are considered rigid in the stress calculation. Details of thermo-mechanical data and thermo-physical data are shown in Figures 4 and 5. Also, thermo-physical data for the shell mold are shown in Table 3. Furthermore, the simulation parameters are listed in Table 4.[18–20] Initial parameters consist of chill plate temperature (20 °C), withdrawal rate (2–5 mm/min), shell mold preheating temperature (1500 °C) and pouring temperature (1550 °C).

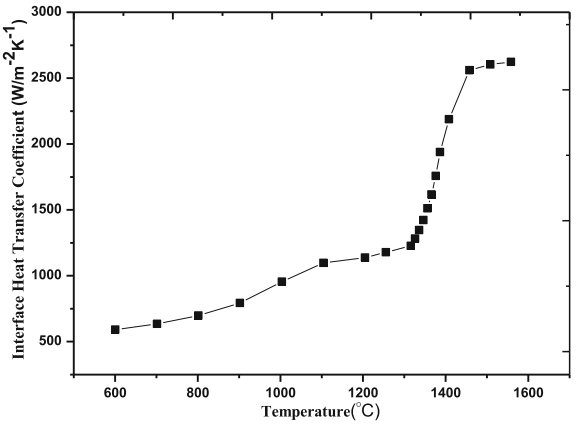

Figure 3. Casting–chill plate interface heat transfer coefficient.

Table 2. DD6 Solidus/Liquidus Temperature

Alloy	Liquidus (°C)	Solidus (°C)	Liquid–solid range (°C)
DD6	1398	1345	53

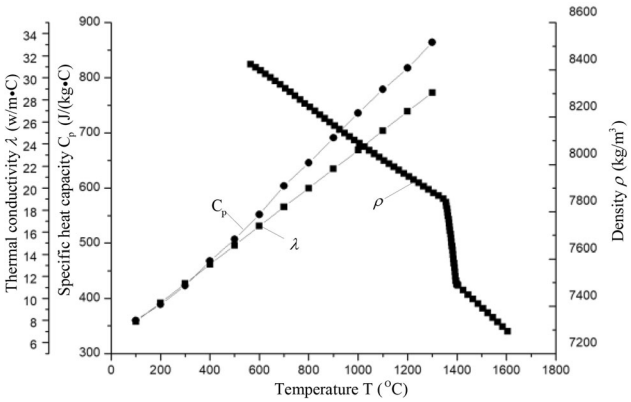

Figure 4. Thermal parameters of DD6.[21]

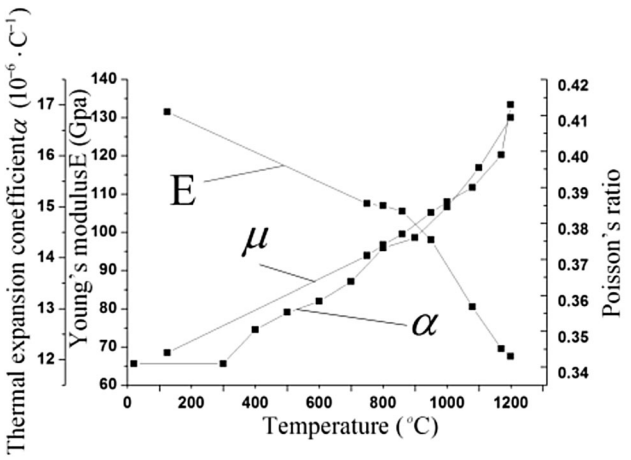

Figure 5. Mechanical properties of DD6.[21]

Table 3. Shell Mold Thermo-physical Parameters

Shell mold	Heat conductivity λ (W m^{-1} K^{-1})	Density ρ (kg m^{-3})	Specific heat C_P (J g^{-1} K^{-1})
Silica sand	0.59	1520	1.2

Process Bar Dimension Determination

Since the cross-sectional area of the platform is not uniform, the stray grain can then easily form at the edge of it. Usually, in order to avoid stray grain defects, the solidification process must be modified with a lower withdrawal rate. However, this method cannot eliminate stray grain defects entirely. Thus, to fully eliminate stray grain defects, the process bar method is used to control strain grain.

FEA simulation was used to determine the position and number of process bar. Normally, the most useful method is CAFÉ method. However, using this method to determine the stray grain position and number of process bar requires precise nucleation parameters, and parameters of SX

Table 4. Model Parameters for FE-Based Solidification Modeling

Thermo-physical properties	
Latent heat	99 kJ kg^{-1}
Interface heat transfer coefficients	
Casting-ceramic	500 W m^{-2} K^{-1}
Boundary conditions	
Shell emissivity	0.5
Baffle emissivity	0.8
Chill plate temperature	20 °C
Run parameters	
FE mesh size	0.5 mm

superalloy cannot be precisely measured by experiment. Therefore, the cooling rate was applied for analysis. Stray grain will not form until cooling rate is beyond the critical value. Otherwise, the stray grain cannot form. To describe the cooling rate of the edge platform, 18 measuring points were set on the two long edges of the plate, which are illustrated in Figure 6.

Cooling rate is calculated at the solid temperature. Since two short edges include connecting structure, the max cooling rate would not appear in these areas. The process bar is then designed at the two long edges of the plate.

Meanwhile, how to determine the dimension of the process bar is still a problem. Considering the operability of the actual manufacturing process, the cross section of process bar that helps in connecting the plate edge is designed as a rectangle. Details of the 3 critical dimensions are shown in Figure 7. (A is process bar extension length, and B and C are the process bar cross section length and width, respectively.) In addition, considering the solidification characteristic of the superalloy, the 3 critical dimensions of

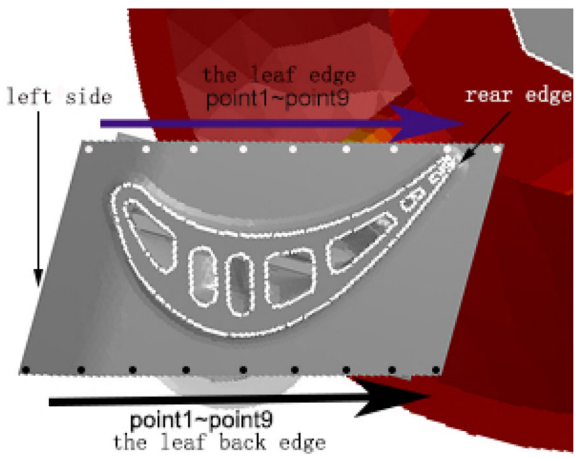

Figure 6. The positions of cooling rate measurement points.

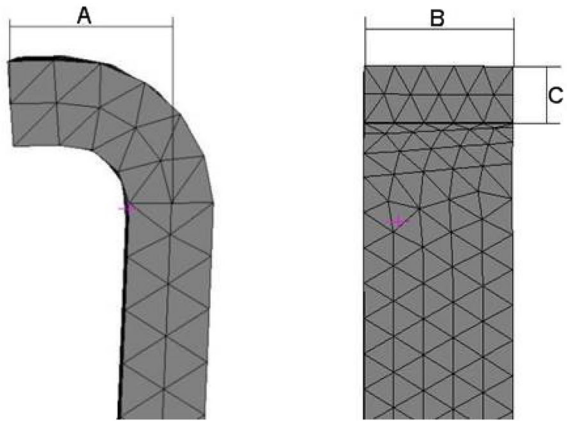

Figure 7. Three critical dimensions of the process bar (A: process bar extension length, B: process bar cross section length, C: process bar cross section width).

the process bar should be limited within small ranges. Since the thickness of platform is 2 mm, the C was set as 2 mm. According to the project, A is limited by the dimension of the chill plate. As shown in Figure 8, the position of the turbine blade limit that B cannot exceed 3.5 mm when the corner area needs to set the process bar. Additionally, the flowing characteristic of the superalloy makes B smaller by 4 mm.

With the analysis of A and C, B becomes the key factor to control the cooling rate of the platform. The main aim of the process bar is to increase the energy to decrease the cooling rate, so the initial value of B cannot be large. In this study, the initial value of B is 5 mm. With the defined A, B and C, the CAE mold was then established.

The Position of the Process Bar Design

Combined with the critical cooling rate, the solidification time map at the edge plate was established according to simulation results, as illustrated in Figure 9, which shows the time when the edge plate region reached the solidus line at different withdrawal rates. The first solidified area near the left side is in close proximity to the side of the

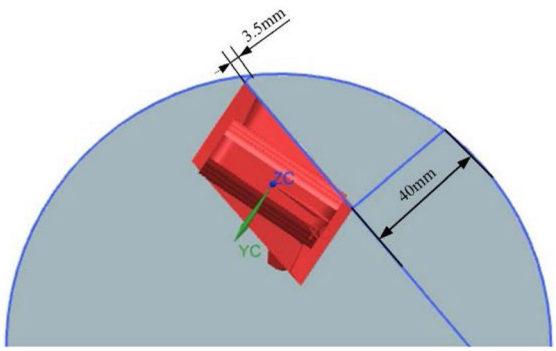

Figure 8. The position of the turbine blade at the chill plate.

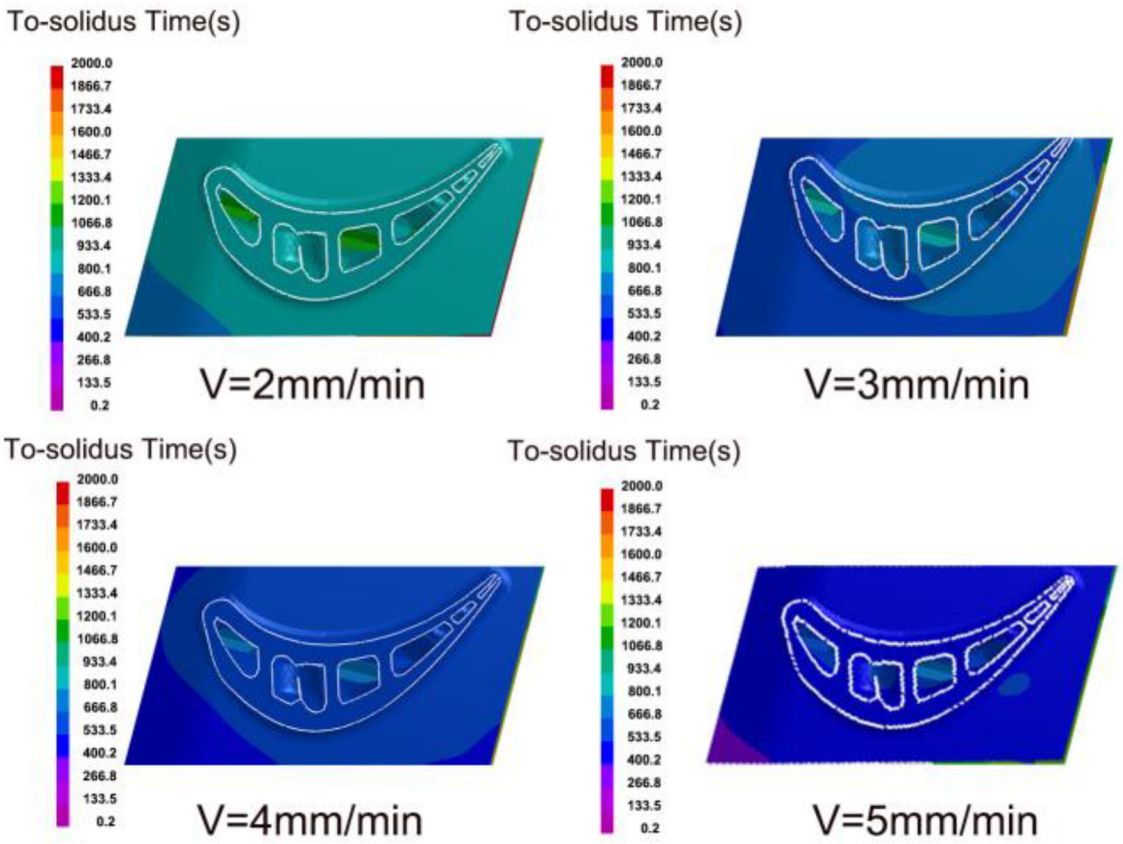

Figure 9. The edge plate section reaches the solidus time at different withdrawal rates.

furnace wall, and then, the solidified area is the rear edge that it is close to the side of the sprue (the whole red area in Figure 6). As the withdrawal rate increased, the time for the edge plate to reach the solidus line near the side of the furnace wall is becoming shorter. Also, since the sections of the edge plate are not on the same plane, there is a certain difference in the time of reaching the solidus line. According to the gating system designed in the blade casting process, the side closer to the furnace wall is lower than that of the rear edge, and it thus further increased the solidification rate of the furnace wall. In addition, when $V \geq 3$ mm/min, time taken to reach the solidus reduced when V increased. This phenomenon indicates that the region (the area under the blue ribbon) is larger where the solidification rate increases as the withdrawal rate grows.

As shown in Figure 10, the cooling rate increases with the withdrawal rates. The cooling rate on the edge of the leaf edge tends to fall along the edge of the leaf edge except point 1 and point 9. However, apart from point 1 and point 9, the cooling rate on the edge of the leaf back edge was at a state in which both sides are high and low in the middle. Compared to the critical cooling rate, the stray grain appeared when the withdrawal rate exceeds 3 mm/min. Also, when the withdrawal rate is 3 mm/min, the stray grain appeared at the back edge of the turbine blade. Therefore, 3 mm/min is the critical withdrawal rate for stray grain condition to occur at both sides of the edge. Thus, this phenomenon demonstrates that the position of the process bar can be determined by numerical simulation.

According to the result of the cooling rate at each point at different withdrawal rates in Figure 10, when $V \geq 3$ mm/min, the edge of the platform deserves three process bars. Positions of those process bars were determined by the cooling rate. When the point's cooling rate is beyond the critical value, the point should be set as the process bar connection area. For this simulation, the V is 4.5 mm/min. According to Figure 10b, the back of the turbine blade deserves process bars. Considering the structure of the platform, the two process bar was set at the assembly structure area. Meanwhile, according to Figure 10a, the basin of the turbine blade needs one process bar and the process bar should be placed at the maximum cooling rate of the assembly structure near the furnace wall.

CAE Modeling

Details of CAE models are shown in Figure 11. In Figure 11a, there is no process bar on the turbine blade. In Figure 11b, there is one process bar on the turbine blade and there are three process bars on the turbine blade for Figure 11c. Additionally, dimensions of the process bar are A = 3.5 mm, B = 5 mm and C = 2 mm.

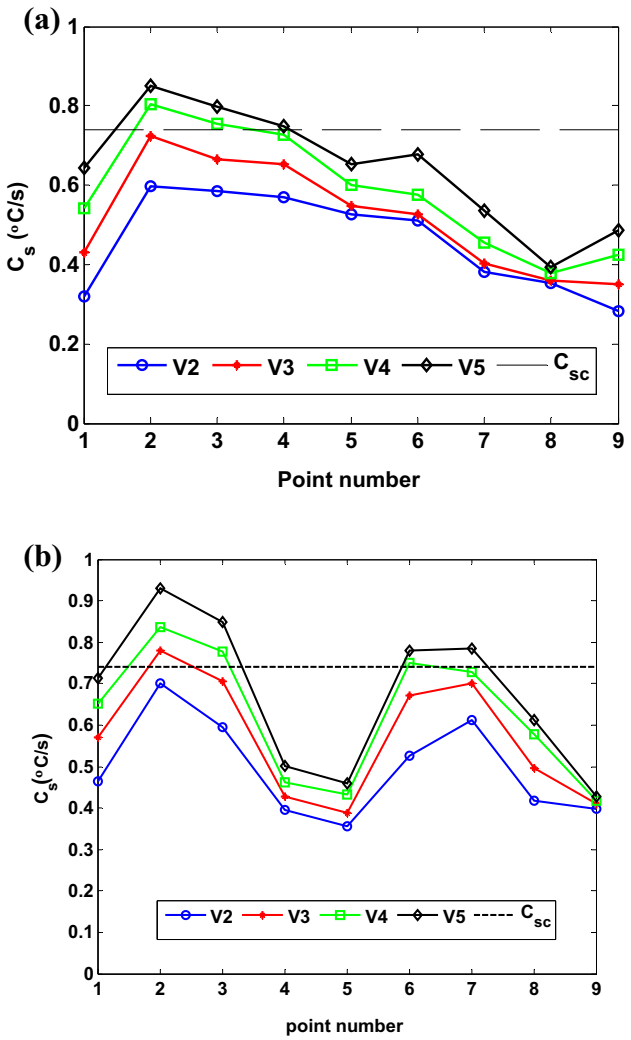

Figure 10. Cooling rate at each point at different withdrawal rates: (a) the leaf edge; (b) the leaf back edge.

The main process parameters for the directional investment casting include the temperature of the furnace high-temperature zone (T_1 = 1500 °C), low-temperature zone temperature (T_2 = 15 °C), withdrawal rate (V = 4.5 mm/min), shell mold preheating temperature (T_3 = 1500 °C) and cold copper temperature (T_4 = 15 °C).

Casting Experimental

According to the simulation results, the casting experiment of turbine blade was developed. Following the sequence of investment casting process, the silicon-based ceramic core was produced and then the core was put into the die with medium temperature die material and pressed by wax press. Then, the casting system, process bar and two wax pattern mold were assembled. Then, the shell mold was produced. Finally, the mold is cast using a Bridgman process furnace. And the whole casting experiment is developed at the AECC Xi'an Aero-Engineer LTD. During the casting experiment, the most important process parameters withdrawal rate is considered. The maximum withdrawal rate was limited by the turbine blade itself. By using this mold, the maximum withdrawal rate is 4.5 mm/min. Thus, with same parameters used in simulation, the withdrawal rate at the edge plates after the addition of the process bar can be up to 4.5 mm/min. The casting mold is shown in Figure 12.

In addition, after the casting experiment, the ceramic core was removed and the process bar was cut by wire cutting. The platform corner was checked by water immersion method. In order to analyze the effect of the process bar, one of the platform corners is cut by wire cutting. The etching solution is HCl(80 ml) + $CuSO_4$(20 g) +

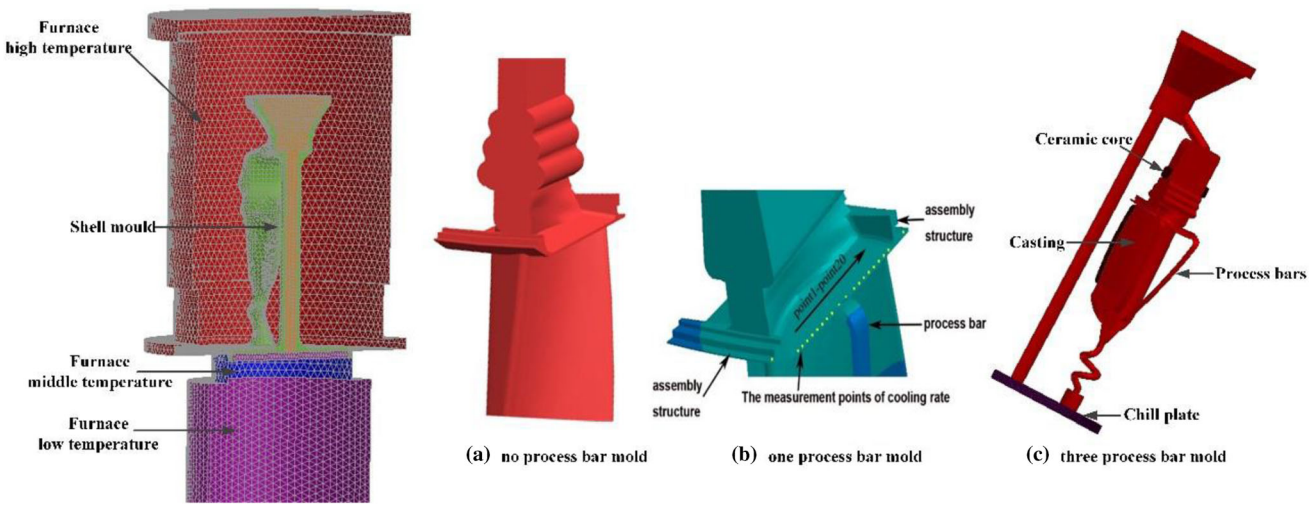

Figure 11. CAE model.

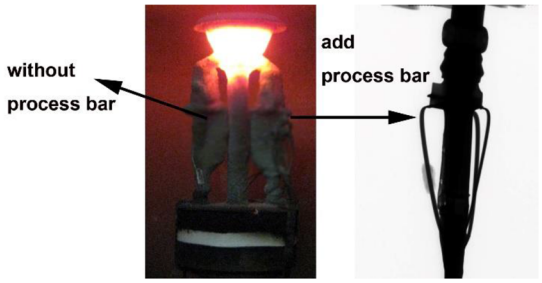

Figure 12. The experimental model.

H_2O(100 ml). And then, it is checked under the optical microscope.

Results and Discussion

The Temperature Field Analysis

Figure 13 shows the temperature field contrast between (a) without process bar and (b) add one process bar at the same time. The result shows the temperature field is almost same at the body of the turbine blade. And the isotherm shows the same shape. It means that adding process bar has little effect on the temperature field of turbine blade. However, the isotherm of the process bar is higher than the body of turbine blade. It seems the process bar could add the cooling rate of the connect area. But unfortunately, the connect area will form a heat barrier area. The heat loss becomes slow during the sequence solidification. Thus, the dendritic has enough time to grow to the platform.

The position of the point1 and point2 is shown in Figure 13. As shown in Figure 14, the temperature–time curve shows the "out of the connect area" (point1) and the "in the connect area" (point2). The point in the "out of the connect area" is clearly ahead of the connect area at the mushy zone. It means the process bar changes the

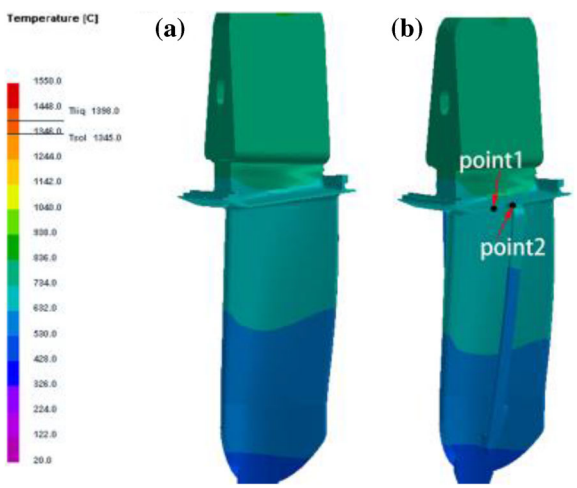

Figure 13. The isotherm of the turbine blade at the same time: (a) without process bar (b) add the process bar.

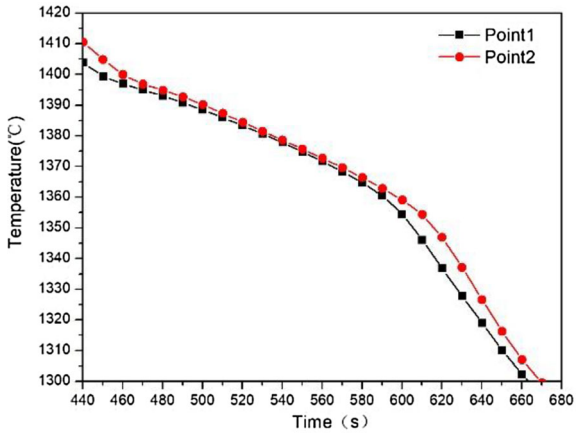

Figure 14. The temperature–time curve shows the out of the connect area (point1) and the point in the connect area (point2).

solidification front and slowly the cooling rate of the connect area.

The Displacement Field Analysis

The deformation result is calculated using Geomagic software. As shown in Figure 13, the two molds are imported in the software and compared with the CAD mold, respectively. Figure 15 shows the turbine blade's edge platform deformation contrast between with a process bar and without a process bar. As shown in the figure, the max deformation occurs at the corner. And the corner is the last to solidify. It is according to the sequence of the solidification. What is more, the shape of the add process bar curve is more stable than the without process bar curve. It means the process bar can optimize the deformation of platform. And this phenomenon is a benefit for the dimension control of the platform.

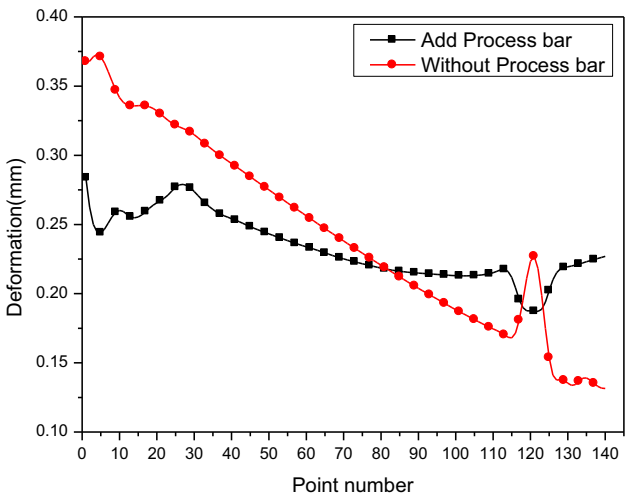

Figure 15. The turbine blade's edge platform deformation contrast between with a process bar and without a process bar.

Control of Stray Grain Formation by Process Bar Method

With the help of the process bar, the cooling rate of the connecting area is reduced, which is due to the process bar that introduced a thermal node, and the heat loss rate is then reduced. Thus, the stray grain can hardly form during the low cooling rate. On the basis of this principle, the single process bar CAE model is established, and the main purpose of this model is to test the effected areas of the process bar. The position of the process bar is set at the middle area, which is illustrated in Figure 11b. In order to analyze the change of cooling rate after adding the process bar, the connecting edge of the plate is divided to 20 points. The cooling rate result of the 20 points is demonstrated in Figure 16.

As shown in Figure 16, the process bar controlling area ranges from point 8 to point 12. The width between point 8 and point 12 is 8 mm, and the whole edge of the platform is 27 mm. Thus, the process bar of B = 5 mm is sufficient to control the cooling rate of the turbine blade.

Distribution of cooling rate after adding three process bars is illustrated in Figure 17. The cooling rate of the process bar connecting area is decreased, and the cooling rate of two edge platforms is all under the critical cooling rate. It means the stray grain is controlled by this process bar method.

Experimental Verification

The macrostructure is shown in Figure 18, and the result shows the process bar is useful to eliminate the stray grain of the platform. As shown in Figure 18a, the dendrite growth orientation (the red line) is shown to be obviously different. And in Figure 18b, the dendrite growth orientation is the same. In order to specifically describe the difference between with a process bar and without a process bar one of the platform corner was cutting, the position of the cutting (the black line area) is shown in Figure 18.

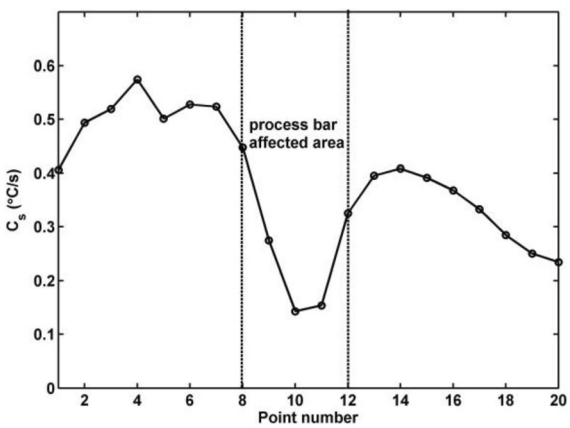

Figure 16. The control area of the process bar.

After the etching, the cutting samples were checked by optical microscope which is shown in Figure 19, the results showed that the stray grain on the edge plates was eliminated. There is obviously grain boundary at the without process bar sample. Thus, the stray grain defects can be effectively controlled by using the process bar.

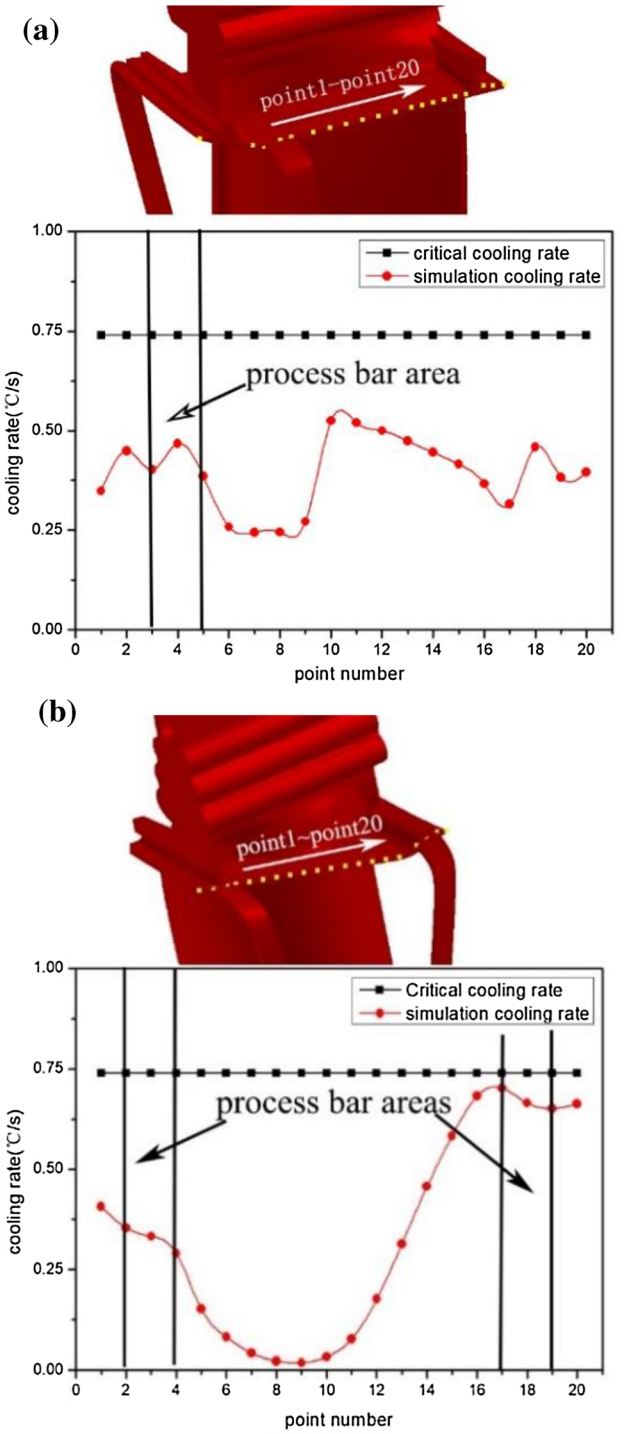

Figure 17. The cooling rate distribution after adding three process bar: (a) cooling rate at each point on the edge of the leaf edge; (b) cooling rate at each point on the edge of the leaf back edge.

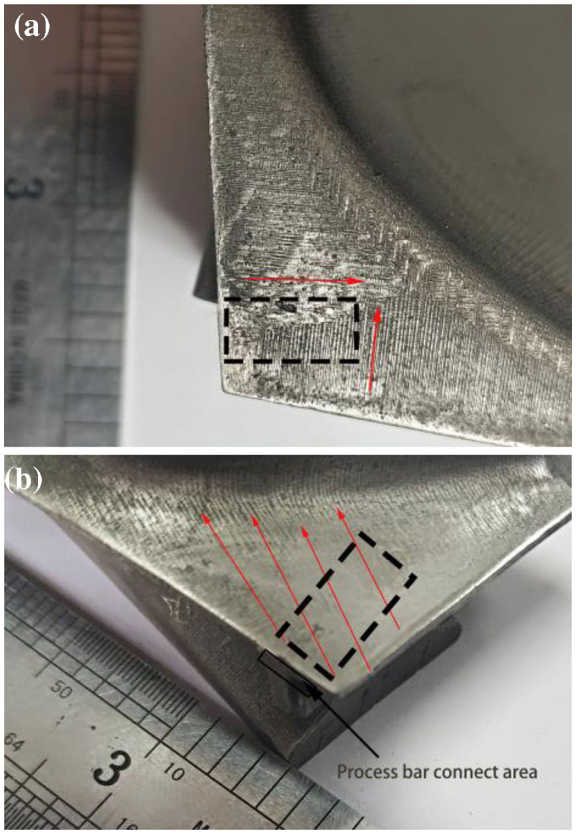

Figure 18. The macrostructure of the turbine blade: (a) the macrostructure of without process bar turbine blade (b) the macrostructure of add process bar turbine blade.

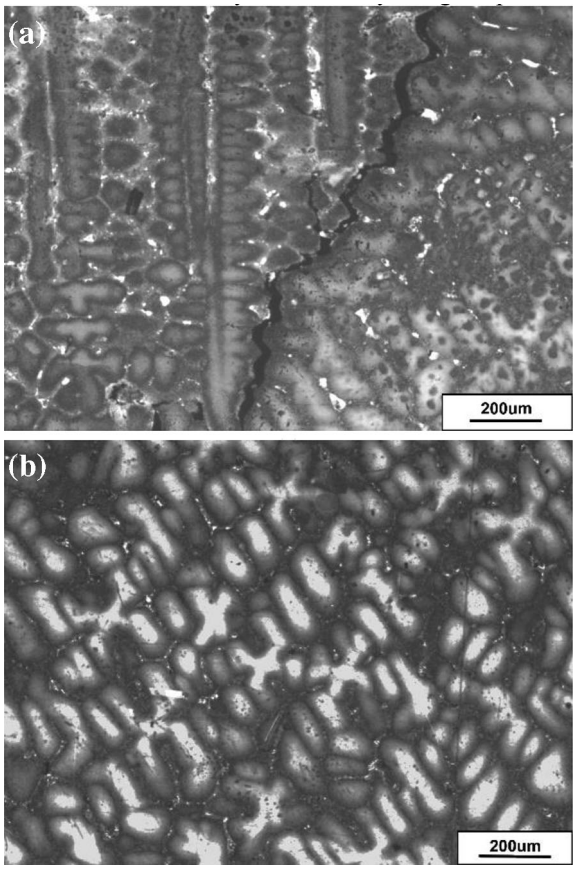

Figure 19. The microstructure of the turbine blade's edge platform (a) without the process bar; (b) add the process bar.

Conclusion

In this study, the process bar was introduced to control the stray grain. With the help of the simulation, the dimension of the process bar was determined, the result of which were compared to that of the experiment. Stray grain was finally eliminated by this method. The results are listed below.

1. The process bar was put forward to control the stray grain, and a method of design the process bar is described. Also, with the help of the simulation, the process bar dimension for this turbine blade is determined, the process bar extension length (A) is 3.5 mm, cross section length (B) is 5 mm, and cross section width (C) is 2 mm.
2. The process bar could modify the shape of the solidification interface, and it could control the dimension of the platform.
3. The process bar method is validated by experiment, and it is useful to control the stray grain during the investment casting. Additionally, the withdrawal rate at the edge plates increased from 2.5 to 4.5 mm/min.

Acknowledgements

This study was co-supported by the National Natural Science Foundation of China (No. 51371152).

REFERENCES

1. G. Shang, P. Gao, F. Luo et al., Effect of Ca on the Y content and cyclic oxidation behavior of Ni-based single-crystal superalloy. Int. J. Metalcast. **12**(3), 607–613 (2018)
2. S.F. Gao, L. Liu, J. Zhang, et al., Simulation of stray grain formation at the platform during Ni-base single crystal superalloy DD403 casting. China Foundry **12**(2), 118–122 (2015)
3. X. Meng, J. Li, Z. Chen et al., Effect of platform dimension on the dendrite growth and stray grain formation in a Ni-base single-crystal superalloy. Metall. Mater. Trans. A **44**(4), 1955–1965 (2013)
4. Jia Y, He L, Zhao Y et al., Determination of undercooling time for stray grain formation of DD11 single crystal superalloy. J. Aeronaut. Mater. **35**(4), 8–15 (2015)

5. J. Gu, C. Beckermann, A. Giamei, Motion and remelting of dendrite fragments during directional solidification of a nickel-base superalloy. Metall. Mater. Trans. A **28**(7), 1533–1542 (1997)
6. Zhao Xinbao, Liu Lin, Yang Chubin et al., Advance in research of casting defects of directionally solidified nickel-based single superalloys. J. Mater. Eng. **37**(1), 93–98 (2012)
7. Z. Liu, H. Sun, F. Xu et al., Parameters determination of grain microstructure prediction for a single crystal casting simulation and its experimental validation. Int. J. Metalcast. **12**(4), 861–869 (2018)
8. D. Ma, A. Bührig-Polaczek, Application of a heat conductor technique in the production of single-crystal turbine blades. Metall. Mater. Trans. B **40**(5), 738–748 (2009)
9. D.X. Ma, Q. Wu, A. Bührig-Polaczek, Undercoolability of superalloys and solidification defects in single crystal components. Adv. Mater. Res. **278**, 417–422 (2011)
10. D. Szeliga, K. Kubiak, G. Jarczyk, The influence of the radiation baffle on predicted temperature gradient in single crystal CMSX-4 castings. Int. J. Metalcast. **7**(3), 17–23 (2013)
11. X. Zhang, Y. Zhou, T. Jin, X. Sun, Study on the tendency of stray grain formation of Ni–based single crystal superalloys. Acta Metall. Sin. **48**(10), 1229–1236 (2012)
12. X.L. Yang, D. Ness, P.D. Lee et al., Simulation of stray grain formation during single crystal seed melt-back and initial withdrawal in the Ni-base superalloy CMSX4. Mater. Sci. Eng., A **413–414**, 571–577 (2005)
13. M.M. Ter Vehn, D. Dedecke, U. Paul et al., Undercooling related casting defects in single crystal turbine blades. Superalloys **1996**, 471–480 (1996)
14. A. De Bussac, C.-A. Gandin, Prediction of a process window for the investment casting of dendritic single crystals. Mater. Sci. Eng., A **237**(1), 35–42 (1997)
15. Y. Li, L. Liu, T. Huang et al., Multi-scale characterization of stray grain in the platform of nickel-base single crystal turbine blade. Vacuum **131**, 181–187 (2016)
16. W. Wang, A. Kermanpur, P. Lee et al., Simulation of dendritic growth in the platform region of single crystal superalloy turbine blades. J. Mater. Sci. **38**(21), 4385–4391 (2003)
17. Y. Dong, K. Bu, Y. Dou et al., Determination of interfacial heat-transfer coefficient during investment-casting process of single-crystal blades. J. Mater. Process. Technol. **211**(12), 2123–2131 (2011)
18. K. Gryc, B. Smetana, M. TkadlečkovÁ, et al., Comparison of thermal analysis results with the theoretical determination of solidus and liquidus temperatures for specific steel grade, in *International Conference on Metallurgy and Materials* (2013), pp. 116–121
19. C. Panwisawas, J. Gebelin, R. Reed, Analysis of the mechanical deformation arising from investment casting of directionally solidified nickel-based superalloys. Mater. Sci. Technol. **29**(7), 843–853 (2013)
20. X. Zhang, S. Xiong, Q. Xu, Numerical methods to improve the computational efficiency of solidification simulation for the investment casting process. J. Mater. Process. Technol. **173**(1), 70–74 (2006)
21. F. Qiu, K. Bu, J.H. Song et al., Dimensional control of nickel-based single crystal turbine blade investment casting by process control optimization. Int. J. Metalcast. **12**(3), 469–479 (2018)